# Robust Energy Management System for a Microgrid Based on a Fuzzy Prediction Interval Model

Felipe Valencia, *Member, IEEE*, Jorge Collado, Doris Sáez, and Luis G. Marín

***Abstract*—Microgrids have emerged as an alternative to alleviate increasing energy demands. However, because microgrids are primarily based on nonconventional energy sources (NCES), there is high uncertainty involved in their operation. The aim of this paper is to formulate a robust energy management system (EMS) for a microgrid that uses model predictive control theory as the mathematical framework. The robust EMS (REMS) is formulated using a fuzzy prediction interval model as the prediction model. This model allows us to represent both nonlinear dynamic behavior and uncertainty in the available energy from NCES. In particular, the uncertainty in wind-based energy sources can be represented. In this way, upper and lower boundaries for the trajectories of the available energy are obtained. These boundaries are used to derive a robust formulation of the EMS. The microgrid installed in Huatacondo was used as a test bench. The results indicated that, in comparison with a nonrobust approach, the proposed formulation adequately integrated the uncertainty into the EMS, increasing the robustness of the microgrid by using the diesel generator as spinning reserve. However, the operating costs were also slightly increased due to the additional reserves. This achievement indicates that the proposed REMS is an appropriate alternative for improving the robustness, against the wind power variations, in the operation of microgrids.**

***Index Terms*—Energy management system (EMS), microgrids, prediction interval, robust control, wind-based power sources.**

## I. Introduction

MICROGRIDS have received considerable attention in recent years because of their capability to alleviate the growing problems in energy supplies. Because the energy sources are often placed near consumption centers (such as factories and communities), large transmission and distribution systems are no longer required. Thus, the power demand is met with a reduced environmental impact. According to [1], a microgrid is a low-voltage grid with a nominal capacity of approximately tens of kilowatts and is primarily composed of loads, renewable nonconventional energy sources (RNCES), and storage systems. As in bulk power systems, the control tasks are performed in a hierarchical manner in microgrids. Specifically, local controllers are used to drive the energy sources to their reference values and a supervisory controller is used to define the reference values of the energy sources according to an objective. The supervisory control is often called an energy management system (EMS). According to [2], the EMS is responsible for the reliable, secure, and economical operation of microgrids in either grid-connected or stand-alone mode. The objectives of the EMS consist of finding the optimal (or near-optimal) commitment and dispatching the available generation units while considering the expected demand and the available energy in the RNCES. Often, the optimality in an EMS is measured with respect to the operating costs. In this paper, the operating costs are assumed as the sum of the diesel consumption and the unattended demand [3]. Here, the diesel consumption includes the diesel used in both generation process and starting up of the generator. Further discussions regarding the features and tasks of EMS in terms of microgrid operation can be found in [4]–[7].

Microgrids have a broad range of application for electrification purposes, and the EMS is the keystone in these applications [4]–[7]. Therefore, it is of considerable importance for the EMS to consider the main phenomena that affect the available energy and demand to achieve the desired features of the grid. This is especially true because the EMS is commonly formulated as an optimization problem in which the prediction of demand and available energy is required. Nevertheless, it has been found that the high uncertainty of the phenomena that influence the available energy in the RNCES make it difficult to include these phenomena in the EMS formulation. Indeed, the following three main options have been identified in the literature for addressing the formulation of EMS in microgrids [2]: 1) real-time optimization; 2) expert systems; and 3) hierarchical control. However, these approaches do not include the uncertainty in the operation of the microgrid. More recently, EMS approaches have been formulated based on a model predictive control (MPC) framework. The principle behind these approaches is to anticipate the expected behavior of both RNCES and demand over a prediction horizon. Given the predicted behavior of the RNCES and the demand, the commitment and dispatch of the units is performed. It is therefore possible to perform activities in advance to improve the robustness of the microgrid. In this paper, robustness refers to the ability of the microgrid to resist a change without changing its previous configuration [8]. Examples of predictive EMS were reported in [3] and [9]–[12]. In particular, in [3], [10], [11], and [13]

Manuscript received October 23, 2014; revised February 15, 2015 and May 26, 2015; accepted July 20, 2015. Date of publication August 16, 2015; date of current version April 19, 2016. This work was supported in part by the Fund for Research Centers in Priority Areas Project Solar Energy Research Center Chile under Grant 15110019, in part by the National Fund for Science and Technology Project 1140775, and in part by the Complex Engineering Systems Institute under Grant ICM: P-05-004-F and Grant CONICYT: FBO16. Paper no. TSG-01061-2014.

The authors are with the Solar Energy Research Center Solar Energy Research Centre-Chile, Department of Electrical Engineering, University of Chile, Santiago 6513027, Chile (e-mail: felipe.valencia@gmail.com).

Color versions of one or more of the figures in this paper are available online at http://ieeexplore.ieee.org.

Digital Object Identifier 10.1109/TSG.2015.2463079

predictive EMS was formulated with the aim of reducing both operating and ancillary costs of the microgrid.

Notwithstanding the improvements in the aforementioned EMS approaches based on MPC, how to address the uncertainty in the RNCES and the demand remains a pressing issue. Due to the nonsmooth behavior of the RNCES, including a prediction model has not been sufficient to ensure the robustness in the operation of microgrids. With the purpose of addressing the pending issues, several robust EMS (REMS) approaches have also been proposed in [14]–[20]. These robust approaches attempted to include the uncertainty in the optimization procedure associated with the EMS. In REMS formulations, two frameworks have been widely used: 1) scenario-based [15], [16]; and 2) stochastic-based approaches [17], [18]. The difference between these two approaches is associated with how the uncertainty is addressed. In scenario-based approaches, diverse operating conditions are considered, and based on these conditions, the unit dispatch is performed. In contrast, in stochastic-based approaches, probability density functions are used to represent the uncertainty in meeting the demand with the expected available energy resources. For examples of scenario-based EMS, consider the approach in [15]. In this approach, all possible operating scenarios were analyzed off-line. For each scenario, an optimal unit commitment was computed. Subsequently, the real-time commitment was performed considering: 1) the operating conditions of the microgrid; 2) the cases previously analyzed; and 3) the optimal solutions obtained for each case. In addition, in [16], a neural network was trained with several optimal power flows (each corresponding to a possible operating scenario). Consequently, depending on the operating conditions of the microgrid, the commitment and dispatch of the units was provided by the neural network without using an on-line optimization procedure. For examples of stochastic-based EMS, consider the work in [17]. Here, the observed mean values and standard deviations of the available data were used to generate stochastic scenarios of solar radiation, wind speed, and load demand. Then, stochastic operating cost optimization models for minimizing the operating costs of the microgrid were formulated. In addition, the probability of self-sufficiency was used in [18] for the commitment and dispatch of the units in a microgrid, specifically, the probability of being able to provide the demanded energy with the energy resources of the grid. In this sense, the power balance equation was changed by the probability of satisfying the demand with the local resources.

Although the aforementioned EMS formulations appear to be a feasible solution for addressing the uncertainty, the computational burden might increase: 1) as the number of cases increases; 2) as the number of RNCES in the microgrid increases; and/or 3) based on the presence of energy storage systems (ESSs) (see [15], [16] for details). Furthermore, selecting the probability density functions for modeling the uncertain terms is not an easy task. Such a selection could also decrease the performance of the EMS and the performance of the microgrid. The decrease in performance results from the differences between the real and the predicted behavior of the uncertain variables. This paper presents a scenario-based EMS developed based on the MPC framework and that is capable of addressing the uncertainty of the RNCES in a microgrid, in which a reduced number of scenarios is considered to model the available energy of the nonconventional energy sources (NCES). For this purpose, fuzzy prediction interval models (FPIMs) were used to predict the available energy of the RNCES. FPIMs are fuzzy models whose outputs are an interval that ensures with a certain coverage probability that the trajectories of the uncertain phenomena belong to the domain defined by the upper and lower boundaries of the interval [21]. In this paper, wind-based energy sources were modeled using the FPIM. The FPIM subsequently provided the upper and lower boundaries for the sources' available energy. Given these boundaries, the unit dispatch was performed. Thus, a significant reduction in the number of scenarios required to include the uncertainty in the EMS was obtained. Furthermore, the computational burden associated with the robust solution of the EMS was also decreased because the FPIM provided information about both worst and best cases (from the perspective of available energy) that the microgrid could experience. Note that the reason for only considering wind-based energy sources was because this paper was developed considering the conditions of the microgrid already installed in Huatacondo [3]. The Huatacondo microgrid was installed in an isolated village in the Atacama Desert, Chile (20° 55' 36.37" S 69° 3' 8.71" W). This system consists of two photovoltaic systems rated at 22 kW in total; a wind turbine with a maximum capacity of 5 kW; the existing 120 kW diesel generator unit of the village; a 40 kW ESS, which is composed of a lead-acid battery bank connected to the grid through a bidirectional inverter; a 1 kW water pump; and a demand-side management system (further details of the microgrid are presented in [3]). Due to the weather conditions where Huatacondo is located, the main source of uncertainty in the operation is the wind-based energy source. The day-to-day variations in the solar radiation are not significant compared to the wind speed variations.

The remainder of this paper is organized as follows. Section II presents the FPIM for the wind-based energy sources. In Section III, the proposed EMS is described. Section IV presents the simulation results. Finally, Section V provides the conclusion.

## II. Fuzzy Model for the Wind-Based Energy Sources

This section formulates the proposed FPIM for wind-based energy sources in a microgrid. Notwithstanding the studies performed to determine the factors that primarily affect wind-based energy production (see [22]), estimating the available energy remains an important task. Let $P_E(t)$ and $v(t)$ denote the wind-based power and the wind speed, respectively. Then, the produced wind-based power is generally expressed as a function of the wind speed to the third power; specifically

$$P_E(t) = k_E v^3(t) \tag{1}$$

where $k_E \in \mathbb{R}$ is constant. Thus, from (1), estimating the available energy from wind-based energy sources requires estimating the wind speed. However, this task is as difficult as

directly estimating the available energy. To overcome these difficulties, in this paper, a fuzzy model whose output is a range rather than a trajectory is proposed. In this way, both dynamics and uncertainty are adequately addressed. In the next sections, the proposed FPIM and its application to the Huatacondo microgrid are presented.

### A. Fuzzy Prediction Interval Models

The proposed FPIM is based on the Takagi–Sugeno (TS) model presented in [23]. This model was selected because of its widely demonstrated capabilities in representing the dynamic behavior of nonlinear systems. In general, TS models have the form (2) [21], where $M_{\mathrm{TS}}$ denotes the number of rules, $x_p(k)$, $x(k)$ denote the vector of premises and the consequences at time step $k$, $\beta_j(x_p(k))$ denotes the normalized activation degree of the $j$th rule, and $\theta_j$ denotes the vector of parameters of the linear model associated with the $j$th rule

$$\hat{y}(k) = \sum_{j=1}^{M_{\mathrm{TS}}} \beta_j(x_p(k))\theta_j^T x(k). \tag{2}$$

In (2), the normalized activation degree satisfies $0 \leq \beta_j(x_p(k)) \leq 1$, $j = 1, \ldots, M$, and $\sum_{j=1}^{M} \beta_j(x_p(k)) = 1$.

At time step $k$, let $z(k) = [x_p^T(k), x^T(k)]^T$ denote the vector of model input variables. The objective of the interval modeling, particularly of the interval fuzzy modeling, is to find functions $\overline{f}(z(k))$ and $\underline{f}(z(k))$ such that $\underline{f}(z(k)) \leq y(k) \leq \overline{f}(z(k))$ (here, the inequality indicates an element-to-element relation). Based on (2), in interval fuzzy modeling, the function $f(z(k))$ is defined as $f(z(k)) := \sum_{j=1}^{M_{\mathrm{TS}}} \beta_j(x_p(k))\theta_j^T x(k)$. Therefore, the interval fuzzy modeling problem becomes one of finding the parameters $\underline{\theta}_j$ and $\overline{\theta}_j$ for each rule such that $\sum_{j=1}^{M_{\mathrm{TS}}} \beta_j(x_p(k))\underline{\theta}_j^T x(k) \leq y(k) \leq \sum_{j=1}^{M_{\mathrm{TS}}} \beta_j(x_p(k))\overline{\theta}_j^T x(k)$ [21]. Next, the FPIM for the wind-based energy sources in a microgrid is described.

### B. Fuzzy Prediction Interval Model for Wind Power

The FPIM derived in this paper for wind-based energy sources considers linear consequences that include both endogenous and exogenous variables. Namely, each consequence is composed of regressors of the wind power (endogenous variable) and the wind speed (exogenous variable). Let $P_E(k)$ and $\nu(k)$ denote the discrete values of $P_E(t)$ and $\nu(t)$, respectively. In addition, let $\hat{P}(k-1) = [P_E(k-1), \ldots, P_E(k-q)]^T$ and $\hat{\nu}(k-1) = [\nu^3(k), \ldots, \nu^3(k-q)]^T$ be the vectors of the regressors of the wind power and the wind speed, respectively. Then, in accordance with the fuzzy model in (2), the model input variables of the proposed FPIM are $z(k) = [\hat{P}^T(k-1), \hat{\nu}^T(k-1)]$. These variables are used to determine to what extent each rule contributed to the output of the model, assuming that $x_p(k) = x(k) = z(k)$ in (2). Hence, the $j$th rule of the TS model of the available energy of the wind-based energy sources is written as follows:

$$\begin{aligned}\mathbf{R_j}: \text{ if } \hat{P}(k-1) \text{ is } A \text{ and } \hat{\nu}(k-1) \text{ is } B \text{ then}\\ P_E^j(k) = -a_{q-1}^j P_E(k-1) - \cdots - a_0^j P_E(k-q)\\ + b_{q-1}^j(\nu(k))^3 + \cdots + b_0^j(\nu(k-q))^3\end{aligned} \tag{3}$$

where $\theta_j = [a_{q-1}^j, \ldots, a_0^j, b_{q-1}^j, \ldots, b_0^j]^T$ [using the same notation as in (2)]. Thus, the prediction model for the available energy of the wind-based energy source is $P_E(k) = \sum_{j=1}^{M_{\mathrm{TS}}} \beta_j(\hat{P}^T(k-1), \hat{\nu}^T(k-1))P_E^j(k)$. Accordingly, let $\underline{P_E}^j(k)$ and $\overline{P_E}^j(k)$ denote the fuzzy models that define the lower and upper boundaries, respectively, of $P_E(k)$. Specifically, they are fuzzy models such that $\underline{P_E}^j(k) \leq P_E(k) \leq \overline{P_E}^j(k)$ for all $k$, whose parameters are $\underline{\theta}^j = [\underline{a}_{q-1}^j, \ldots, \underline{a}_0^j, \underline{b}_{q-1}^j, \ldots, \underline{b}_0^j]^T$ for $\underline{P_E}^j(k)$ and $\overline{\theta}^j = [\overline{a}_{q-1}^j, \ldots, \overline{a}_0^j, \overline{b}_{q-1}^j, \ldots, \overline{b}_0^j]^T$ for $\overline{P_E}^j(k)$. The sets of parameters $\underline{\theta}^j$ and $\overline{\theta}^j$ are obtained through the solution of the optimization problems (4) (for the lower boundary) and (5) (for the upper boundary). In both cases, $P_{Ei}(k)$ denotes the real (measured) value of the wind power. Moreover, the constraints $P_{Ei}(k+h) - \sum_{j=1}^{M_{\mathrm{TS}}} \beta_j\big(x_p(k+h-1)\big)\underline{P_E}^j(k+h) \geq 0$ (for the lower boundary) and $P_{Ei}(k+h) - \sum_{j=1}^{M_{\mathrm{TS}}} \beta_j\big(x_p(k+h-1)\big)\overline{P_E}^j(k+h) \leq 0$ (for the upper boundary) are included to ensure that the relation $\underline{P_E}^j(k) \leq P_E(k) \leq \overline{P_E}^j(k)$ is satisfied by the FIPM over the prediction horizon $N_p$ (throughout the paper, the abbreviation s.t refers to the expression subject to)

$$\begin{aligned}&\min_{\underline{\theta}_j, t_1} \ t_1\\ &\text{s.t:}\\ &P_{Ei}(k+h) - \sum_{j=1}^{M_{\mathrm{TS}}} \beta_j\big(x_p(k+h-1)\big)\underline{P_E}^j(k+h) \leq t_1\\ &P_{Ei}(k+h) - \sum_{j=1}^{M_{\mathrm{TS}}} \beta_j\big(x_p(k+h-1)\big)\underline{P_E}^j(k+h) \geq 0\\ &\underline{P_E}^j(k+h) = \underline{a}_{q-1}^j P_E^j(k+h-1) + \ldots + \underline{a}_0^j P_E^j(k+h-q)\\ &\qquad + \underline{b}_{q-1}^j(\nu(k+h))^3 + \ldots + \underline{b}_0^j(\nu(k+h-q))^3\\ &t_1 \geq 0, \quad h = 1, \ldots, N_p\end{aligned} \tag{4}$$

$$\begin{aligned}&\min_{\overline{\theta}_j, t_2} \ t_2\\ &\text{s.t:}\\ &\sum_{j=1}^{M_{\mathrm{TS}}} \beta_j\big(x_p(k+h-1)\big)\overline{P_E}^j(k+h) - P_{Ei}(k+h) \leq t_2\\ &P_{Ei}(k+h) - \sum_{j=1}^{M_{\mathrm{TS}}} \beta_j\big(x_p(k+h-1)\big)\overline{P_E}^j(k+h) \leq 0\\ &\overline{P_E}^j(k+h) = \overline{a}_{q-1}^j P_E^j(k+h-1) + \ldots + \overline{a}_0^j P_E^j(k+h-q)\\ &\qquad + \overline{b}_{q-1}^j(\nu(k+h))^3 + \ldots + \overline{b}_0^j(\nu(k+h-q))^3\\ &t_2 \geq 0, \quad h = 1, \ldots, N_p.\end{aligned} \tag{5}$$

Note that the optimization problems (4) and (5) are formulated only for parameter identification. To determine the structure of the models (that is, the number of rules and the relevant variables) of the FPIM, the methodology in [24] is used. From this methodology, the same structure is obtained for both $\underline{P_E}^j(k)$ and $\overline{P_E}^j(k)$. Therefore, the models composing the FPIM for the available energy of the wind-based energy sources only differed in the values of their consequence parameters.

Additionally, note that the optimization problems (4) and (5) are based on the insights of the method reported in [21]. In this method, an optimization-based methodology was derived to identify an interval TS model. However, the approach in [21] did not consider a prediction horizon. In this sense, FPIM is an extension of the interval fuzzy models originally presented in [21].

### *C. Fuzzy Prediction Interval Model for the Huatacondo Microgrid*

In this section, the proposed FPIM is identified using the data of the microgrid installed in Huatacondo. The dataset used in the identification procedure corresponds to the period from July 27th to September 26th of 2010. The training dataset corresponds to July 27th to August 26th, the test dataset corresponds to August 27th to September 10th, and the validation dataset corresponds to September 11th to September 26th of 2010. The dataset used in the identification procedure was also composed of two different data types: 1) the wind power produced during the analyzed period; and 2) the estimated wind speed. The estimated wind speed data were included because the solution to the optimization problems (4) and (5) requires the trajectory of the wind speed over the prediction horizon $N_p$. The estimation of the wind speed was performed using a mesoscale model of the region where Huatacondo is located.

From the available dataset, both an FPIM and a fuzzy predictive model were identified. The fuzzy model is included for comparison purposes. This model was implemented in the EMS and used as a baseline for comparisons of the performance of the proposed REMS (see Sections III and IV for more details). From the data, an optimal structure consisting of four rules and two regressors of both $P_E(k)$ and $v(k)$ is obtained. Specifically, $\hat{P}(k-1) = [P_E(k-1), P_E(k-2)]^T$ and $\hat{v}(k-1) = [(v(k))^3, (v(k-1))^3]^T$. Thus, the $j$th rule of the FPIM is as follows:

$$\begin{aligned}\mathbf{R_j}: &\text{ if } P(k-1) \text{ is } A_j^1 \text{ and } P(k-2) \text{ is } A_j^2 \text{ and } (v(k))^3 \text{ is } B_j^1\\ &\text{and } (v(k-1))^3 \text{ is } B_j^2, \text{ then}\\ &\overline{P_E}^j(k) = \overline{a}_0^j + \overline{a}_1^j P(k-1) + \overline{a}_2^j P(k-2) + \overline{b}_0^j (v(k))^3\\ &\qquad + \overline{b}_1^j (v(k-1))^3\\ &\underline{P_E}^j(k) = \underline{a}_0^j + \underline{a}_1^j P(k-1) + \underline{a}_2^j P(k-2) + \underline{b}_0^j (v(k))^3\\ &\qquad + \underline{b}_1^j (v(k-1))^3.\end{aligned}$$

Note that during tuning of the FPIM, a prediction horizon $N_p = 1$ was considered. However, the performance of the interval model was evaluated considering 96-step-ahead predictions. This selection corresponded to a one-day-ahead prediction of the available energy of the wind-based energy sources because a sampling time of 15 min was considered in the application. Furthermore, Gaussian fuzzy membership functions of the fuzzy sets $\mu_j^i(x) = \exp^{-0.5(\gamma_{ij}(x-\sigma_{ij}))^2}$, $i = 1, \ldots, 4$ are also considered in this paper. Here, $i$ indicates the fuzzy set, and $j$ denotes the rule.

Fig. 1(a) shows the comparison between the measured and estimated power, and Fig. 1(b) presents the interval defined by the proposed FPIM. The data presented in these figures correspond to the five days of the validation dataset. For the fuzzy prediction model, the root-mean-squared errors associated with the estimation of $P_E(k)$ are 0.6361 kW with respect to the training dataset, 0.9995 kW with respect to the validation dataset, and 0.8325 kW with respect to the test dataset. These deviations correspond to 18.17%, 28.56%, and 23.76% of the maximum power provided by the wind-based energy source. These errors indicate that the uncertainty in the wind-speed estimation significantly affected the capability of the fuzzy model to predict the behavior of $P_E(k)$, which is also evident in Fig. 1(a). Indeed, the estimated values of $P_E(k)$ obtained with the fuzzy model only provide the expected trajectory of $P_E(k)$. Therefore, the need to use the proposed FPIM for the available energy of the wind-based energy sources is enhanced. Moreover, in the validation set, the FPIM achieved a coverage probability of 95.9449% for 96 step-ahead predictions. Specifically, less than 5% of the measured values were outside the range defined by the predictions made using the proposed interval model. This is evident in Fig. 1(b), in which almost all of the measured values lie inside the range defined by the FPIM. Thus, the effectiveness of the FPIM is confirmed. Furthermore, thanks to the obtained coverage probability, an adequate representation of the uncertainty is also obtained. Thus, the proposed FPIM is suitable for REMS applications. In the next section, the formulation of the REMS is presented.

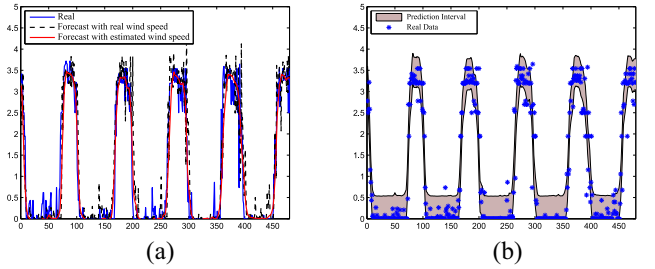


Fig. 1. Measured and estimated wind speed and wind-based power and proposed FPIM for the available energy in the wind-based energy sources of the Huatacondo microgrid. One-day-ahead (a) wind power estimation and (b) FPIM for the wind-based energy.

## III. Robust Energy Management System

This section formulates the proposed REMS based on the FPIM derived in Section II for the available energy of wind-based energy sources. The proposed EMS is based on the EMS reported in [3]. In the approach proposed in this paper, the MPC framework is selected because it is possible to ensure that the current dispatch of the units does not compromise the energy resources in the future. However, due to the intermittent behavior of NCESs, such as wind-based energy sources, the MPC framework might not be sufficient to guarantee an adequate operation of the microgrid. Therefore, the use of the FPIM motivates a new REMS. Indeed, as shown in Section II, the FPIM can model both dynamic behavior and uncertainty of $P_E(k)$. Thus, by combining the MPC framework with the prediction intervals, the robustness of the grid is enhanced.

From Section II, the proposed FPIM provides upper and lower boundary functions for the available wind energy in the microgrid. These boundary functions are interpreted (in the REMS) as the best and worst-case operating conditions, respectively, from the perspective of available energy. Therefore, it is possible to explicitly include the uncertainty into the unit dispatch of a microgrid. Moreover, the proposed REMS considered: 1) the energy that wind- and solar-based sources were able to provide at a given time; 2) the expected demand; and 3) the uncertainty in the available energy from the wind-based energy sources to define the power set-points of each dispatchable generation unit, namely (in the case analyzed in this paper), the diesel generator and the ESS. With the inclusion of the uncertainty in the NCES, a better use of the energy sources was achieved in addition to the enhancement of the robustness of the microgrid.

As is well known, the objective of the dispatch of the units is to minimis the operating costs. In the microgrids analyzed in this paper, the operating costs include the diesel consumption and the unserved energy. The diesel consumption consists of the consumption itself due to the generation process plus the starting up of the generation unit. The unserved energy is related to the amount of the demanded energy the microgrid was not able to supply with the energy resources at a given time. Let $C(k)$ and $C_S(k)$ denote the cost related to the diesel consumption and the cost of starting up the diesel generator, respectively. Let $P_{\mathrm{NS}}(k)$ denote the unserved energy, and let $T_s$ and $N_p$ denote the sampling time and the prediction horizon, respectively. Then, the dispatch of the units in a microgrid is formulated for $h = 1, \ldots, N_p$ as in [3]

$$\min_{\substack{P_D(k+h),P_B(k+h)\\ P_{\mathrm{Lo}}(k+h),S_L(k+h)}} T_s \sum_{h=1}^{N_p} C(k+h) + T_s \sum_{l=h}^{N_p} C_S(k+h) + C_{\mathrm{NS}} T_s \sum_{h=1}^{N_p} P_{\mathrm{NS}}(k+h)$$

s.t:

$$\begin{aligned}
&P_D(k+h) + P_I(k+h) + P_S(k+h) + P_E(k+h) + P_{\mathrm{NS}}(k+h) = P_L(k+h) - P_{\mathrm{Lo}}(k+h)\\
&V_D^{\min} \le V_D(k+h) \le V_D^{\max}\\
&E^{\min} \le E(k+h) \le E^{\max}\\
&S_L^{\min} \le S_L(k+h) \le S_L^{\max}\\
&P_D(k+h),\ P_{\mathrm{NS}}(k+h) \ge 0\\
&P_{\mathrm{Lo}}(k+h) \le 0
\end{aligned} \tag{6}$$

where $P_D(k+h)$, $P_B(k+h)$, and $S_L(k+h)$ denote the diesel reference power, the battery reference power, and the demand signal for the consumers, respectively; $P_S(k+h)$, $P_E(k+h)$, and $P_L(k+h)$ denote the predicted solar power, wind power, and demand, respectively; $P_I(k)$ and $P_{\mathrm{Lo}}(k)$ are the power provided by the inverter and the unused power, respectively; $V_D(k)$ and $E(k)$ are the volume of diesel fuel and the battery energy, respectively; $V_D^{\min}$, $E^{\min}$, and $S_L^{\min}$ are the minimum allowable values for the diesel volume, for the battery energy, and for the customers signal, respectively; and $V_D^{\max}$, $E^{\max}$, and $S_L^{\max}$ are the maximum allowable values for the diesel volume, for the battery energy, and for the customers signal, respectively.

In (6), as in [3], the cost related to the diesel consumption is computed based on the efficiency curve of the generator. From this curve, the amount of diesel required to generate a defined power is determined. Hence, the cost is computed by multiplying the amount of diesel used by the cost-per-liter of diesel. From the same curve, the volume of diesel remaining after each execution of the EMS is also estimated. Additionally, because the generator cannot be restarted after being turned off until a defined time has elapsed, binary variables indicating whether the diesel generator was switched off and how long it was off are included. With these variables, the constraints regarding the elapsed time between a switch off and a turn on are taken into consideration in the EMS. With respect to the operation of the battery, the charging curve is approximated. This curve indicates how much power is required in the charging process as a function of the depth of the discharge. Binary variables are used to represent the constraints regarding the charging process of the battery bank. Additionally, considering that complete depletion of the battery is undesirable, the amount of energy remaining in the battery bank is estimated. The parameters of the microgrid and the values of the costs for the consumption and starting up of the diesel generator and the cost of the unserved power are in [3].

Note that the solution of the optimization problem in (6) depends on: 1) the available energy forecasting and 2) the prediction of the demand. This dependence is reflected in the power balance constraint of the optimization problem (6). From this constraint, the unserved power is written in terms of the remaining variables as

$$\begin{aligned}
P_{\mathrm{NS}}(k+h) = {} & P_L(k+h) - P_{\mathrm{Lo}}(k+h) - P_D(k+h)\\
& - P_I(k+h) - P_S(k+h) - P_E(k+h).
\end{aligned} \tag{7}$$

It is also worth noting that minimizing $P_{\mathrm{NS}}(k)$ in (6) seeks for the achievement of the power balance in the grid. Though the value of $P_{\mathrm{NS}}(k)$ is included in (6) as a costs, its value could also be interpreted as a performance indicator. Considering the relation between $P_E(k)$ and $P_{\mathrm{NS}}(k)$ given by (7), the uncertainty in the forecasting of the available energy of the wind-based energy sources also affects the amount of unserved power and thus the term $C_{\mathrm{NS}} T_s \sum_{h=1}^{N_p} P_{\mathrm{NS}}(k+h)$ in the optimization problem (6). Note that in this paper: 1) the demand forecasting model in [25] and 2) models for the remaining elements in the microgrid used in [3] were considered. Due to the weather conditions of Huatacondo, only uncertainty in the wind-based energy sources is assumed. Thus, the FPIM derived in Section II for $P_E(k)$ is used as the prediction model. Consequently, the expressions (8) and (9) are obtained. These expressions are used in the upper and lower boundaries, respectively, of $P_E(k)$ (defined by the FPIM) in (7)

$$\begin{aligned}
\overline{P}_{\mathrm{NS}}(k+h) = {} & P_L(k+h) - P_{\mathrm{Lo}}(k+h) - P_D(k+h)\\
& - P_I(k+h) - P_S(k+h) - \overline{P}_E(k+h)
\end{aligned} \tag{8}$$

$$\begin{aligned}
\underline{P}_{\mathrm{NS}}(k+h) = {} & P_L(k+h) - P_{\mathrm{Lo}}(k+h) - P_D(k+h)\\
& - P_I(k+h) - P_S(k+h) - \underline{P}_E(k+h).
\end{aligned} \tag{9}$$

Note that depending on the values of $\overline{P}_E(k+h)$ and $\underline{P}_E(k+h)$, there are several values associated with the unserved power cost. Specifically, the FPIM also defines upper and lower boundaries for the costs associated with the unserved power. For instance, consider the following three cases that were used to support the previous claim.

1) When both $\overline{P}_E(k+h)$ and $\underline{P}_E(k+h)$ (plus the contribution of the remaining energy sources) are sufficient to satisfy the demand. In this case, according to (8) and (9), the value of the unserved power is zero, and thus, the cost of the unserved power is also zero.
2) When only $\underline{P}_E(k+h)$ (plus the contribution of the remaining energy sources) is not sufficient to satisfy the demand. In this case, in accordance with (8) and (9), there are two different values for the unserved power, namely, a value of zero associated with $\overline{P}_{\mathrm{NS}}(k+h)$ and a value greater than zero associated with $\underline{P}_{\mathrm{NS}}(k+h)$ (this value, of course, depends on the amount of unserved power).
3) When $\overline{P}_{\mathrm{NS}}(k+h)$ (plus the contribution of the remaining energy sources) is not sufficient to satisfy the demand. In this case, in agreement with (8) and (9), and as in the second case, the unserved power exhibits two different values: one value associated with the value of $\overline{P}_{\mathrm{NS}}(k+h)$ and another value associated with $\underline{P}_{\mathrm{NS}}(k+h)$. In addition, in this particular case, both unserved cost values are greater than zero and depend on the amount of unserved power under each operating condition.

Furthermore, note that the use of the FPIM (derived in Section II) in the dispatch of the units in a microgrid made the proposed approach robust. Moreover, the difference between the proposed approach and the approach presented in [3] lies in the use of: 1) the FPIM as a prediction model; and 2) different scenarios including the uncertainty into the unit dispatch. In addition, each previously analyzed case provided a particular unit dispatch, that is, a particular solution of the optimization problem (6). Accordingly, different trajectories for the decision variables $P_D(k+h), P_B(k+h), P_{\mathrm{Lo}}(k+h)$, and $S_L(k+h),\ h=1,\ldots,N_p$ are obtained. Recall that the FPIM provided the worst- and best-case scenarios for the available energy. In this manner, by performing separate computations of the solution of (6) [one considering $P_E(k)=\underline{P}_E(k)$ and another considering $P_E(k)=\overline{P}_E(k)$], a robust solution for the unit commitment in microgrids is achieved. Here, this solution is approximated by a convex sum of the best- and worst-case solutions

$$P_D^*(k)=\alpha_D\overline{P}_D^*(k)+(1-\alpha_D)\underline{P}_D^*(k) \tag{10}$$

$$P_B^*(k)=\alpha_B\overline{P}_B^*(k)+(1-\alpha_B)\underline{P}_B^*(k) \tag{11}$$

$$P_{\mathrm{Lo}}^*(k)=\alpha_{\mathrm{Lo}}\overline{P}_{\mathrm{Lo}}^*(k)+(1-\alpha_{\mathrm{Lo}})\underline{P}_{\mathrm{Lo}}^*(k) \tag{12}$$

$$S_L^*(k)=\alpha_L\overline{S}_L^*(k)+(1-\alpha_L)\underline{S}_L^*(k) \tag{13}$$

where $P_D^*(k), P_B^*(k), P_{\mathrm{Lo}}^*(k)$, and $S_L^*(k)$ are the optimal values of the decision variables; $\overline{P}_D^*(k), \overline{P}_B^*(k), \overline{P}_{\mathrm{Lo}}^*(k)$, and $\overline{S}_L^*(k)$ are the optimal values of the decision variables considering $P_E(k)=\overline{P}_E(k)$; and $\underline{P}_D^*(k), \underline{P}_B^*(k), \underline{P}_{\mathrm{Lo}}^*(k)$, and $\underline{S}_L^*(k)$ are the optimal values of the decision variables, given $P_E(k)=\underline{P}_E(k)$; and $\alpha_D, \alpha_B, \alpha_{\mathrm{Lo}}$, and $\alpha_L \in [0,\ 1]$ are constants. Fig. 2 presents the block diagram of the proposed REMS. As previously mentioned, the historical values of both wind power $\hat{P}(k-1)$ and wind speed $\hat{v}(k-1)$, as well as their current measured values, $P_E$ and $v_E$, are used as inputs of the FPIM. The FPIM provides the upper, $\overline{P}_E$, and lower, $\underline{P}_E$, values for the wind power predictions. These values, along with the prediction of the solar power, $P_S$, and the load, $P_L$, are the inputs of the EMS. The EMS is composed of two MPC-based optimizers that, in parallel, compute the optimal dispatch of the units, $[\overline{P}_D^*, \overline{P}_B^*, \overline{P}_{\mathrm{Lo}}^*, \overline{S}_L^*]^T$ and $[\underline{P}_D^*, \underline{P}_B^*, \underline{P}_{\mathrm{Lo}}^*, \underline{S}_L^*]^T$, considering separately the values of $\overline{P}_E$ and $\underline{P}_E$, respectively. Given the solution of these optimal unit dispatches, the convex sum indicated in (10)–(13) is performed to obtain the final robust dispatch. Since $\overline{P}_E(k)$ and $\underline{P}_E(k)$ represent with a confidence level of 95% any realization of $P_E(k)$, the dispatch given by (10)–(13) is robust with the same confidence level to the variations in the wind power generation. Note that because the systems are generally not operating all the time under the worst-case scenario, the robust controllers might be more conservative than necessary. Indeed, the microgrids analyzed in this paper are not always performing under the conditions predicted by $\underline{P}_E(k)$. Therefore, always considering the worst-case conditions in their operation could affect their performance in terms of: 1) operating costs; 2) quality of service; and/or 3) response in the presence of disturbances. Thus, the convex combination of the worst-case and best-case optimal solutions is the alternative proposed in this paper to overcome the aforementioned issues regarding the robust formulation of the EMS and, in general, of the robust control problem. However, computing the optimal power dispatch as a convex combination of the solutions given by the best-case and worst-case scenarios requires the selection of a value for the weighting factors $\alpha_D, \alpha_B, \alpha_{\mathrm{Lo}}$, and $\alpha_L$. In this paper, $\alpha_D, \alpha_B, \alpha_{\mathrm{Lo}}$, and $\alpha_L$ are each set to 0.5. Nonetheless, nonsupervised learning strategies or any other technique for on-line parameter selection based on historical data can be used to find an adequate value for this weighting factor. Because selecting the values of $\alpha_D, \alpha_B, \alpha_{\mathrm{Lo}}$, and $\alpha_L$ is beyond the scope of this paper, such an analysis is not included. In the next section, the results obtained using the proposed EMS are analyzed and discussed.

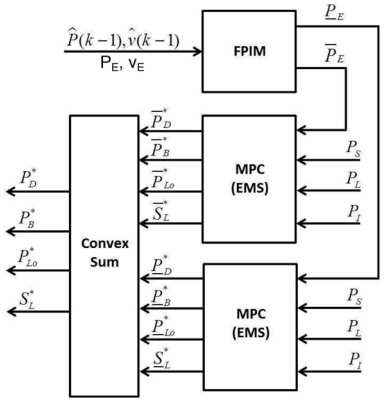


Fig. 2. Block diagram of the proposed REMS.

TABLE I
COMPARISON OF THE OPERATING COSTS BETWEEN THE REMS AND THE CURRENTLY INSTALLED EMS IN THE HUATACONDO MICROGRID

| | Start Up Costs | | Operating Costs | | Total Costs | |
|---|---|---|---|---|---|---|
| | REMS | EMS | REMS | EMS | REMS | EMS |
| Day: | | | | | | |
| 1 | 4000 | 4000 | 35707 | 33070 | 39707 | 37070 |
| 2 | 4000 | 3000 | 36508 | 36872 | 40508 | 39572 |
| 3 | 4000 | 3000 | 36606 | 36780 | 40606 | 39780 |
| 4 | 4000 | 3000 | 35337 | 32731 | 39337 | 35731 |
| 5 | 4000 | 4000 | 38433 | 37468 | 42433 | 41468 |

## IV. SIMULATION RESULTS

This section presents the results obtained using the proposed REMS. As in [3], the microgrid previously installed in Huatacondo is used for the assessment of the REMS. In addition, the EMS in [3] is used as a baseline to compare the performance of the microgrid with the proposed REMS. The test of the REMS was performed over the course of five weeks. During this period, the EMS was performed every 15 min, and both current measurements and historical data were considered in the solution of the unit dispatch problem. Furthermore, because the unit dispatch problem was formulated under the rolling-horizon framework, a prediction horizon of $N_p = 192$ was considered. Such a prediction horizon corresponds to two-day-ahead forecasting, given the frequency with which the EMS was performed. Table I shows the operating costs obtained with the REMS (REMS in the table) and with the EMS in [3] (EMS in the table).

As shown in this table, in terms of the operating costs, the robust approach was 3.4% more costly on average than the EMS. The maximum difference in cost between the two systems occurred during the first week, when the operating costs of the REMS were 7.97% greater, whereas the minimum difference occurred during the second week, when the EMS reduced the operating cost by 1% with respect to the EMS. Although a reduction in the operating costs was achieved during weeks two and three, the REMS maintained the same start-up costs. By contrast, the same costs for the EMS changed from 4000 to 3000. Therefore, as shown in Table I, the total costs for the REMS were always greater than the total costs for the EMS. Specifically, the average increase in the total costs due to the use of the REMS was approximately 4.8%, and the maximum and minimum increases in the costs, with respect to the costs of the EMS, were 10.1% and 2.1%, respectively. The increase in the total costs is consistent with the increase in the use of the diesel generator. The EMS uses the generator to maintain the power balance in the grid when the RNCES plus the ESS are not able to provide the demanded power, whereas the REMS also uses the generator as a spinning reserve to counteract the variations in the wind power.

Fig. 3 presents a comparison between the diesel reserves with the REMS and with the EMS. The reserves were computed as the difference between the rated power of the diesel generator and the power currently supplied, only when the generator was started up. As shown in the figure, every week during the test, the REMS started up the diesel generator four times, whereas the EMS started up the generator 3 or 4 times, depending on the predicted available energy. For the additional start up of the generator, the REMS assigned a power near to 10 kW which is significantly lower than the rated power of the generator. This power assignment allowed to the REMS counteracts the variability of the wind power generation. In fact, for the same reason, during the whole experiment the REMS started up and/or turned off the generator before/after the EMS with a low power assignment. In the figure, it can be seen that the maximum reserve obtained with the EMS was 100 kW, whereas the REMS reached 110 kW which implies an increase of 10% in the reserves. Given the additional use of the diesel generator and in accordance with the definition of robustness provided in the Introduction (see [8]), the additional starting up of the diesel generator improves the robustness in the microgrid because, without changing the transmission capacity, with a confidence level of 95% the microgrid is able to support the variations in the wind power, increase the probability of providing electric energy to the customers, and supply the demanded power despite the variability in the wind power. The confidence level is given by the extent to which the interval model is able to represent the wind power and its associated uncertainty. In this case, as shown in Section II-C the proposed model achieved a confidence level of 95.9449%.

There is another important issue to discuss regarding Table I: the possibility of reducing the operating costs with the use of the REMS. The costs depend on how close the real operating conditions are to the predictions made by the models used to estimate the available energy on the microgrid. Table II presents a comparison of the total operating costs associated with the solution of the unit commitment using different prediction models. Particularly, the upper and lower boundary models composing the proposed FPIM are presented, as well as the EMS, in [3] using the fuzzy model analyzed in Section II. In this table, the label "total cost per week" refers to the average operating cost throughout each week of the test; the labels "lower" and "upper" refer to the predictions made by the lower and upper boundary models of the FPIM, respectively; and the "error" label refers to the average deviation of the predictions from the real-operating conditions. Because neither quadratic nor absolute errors are used, the errors shown in Table II have positive and negative values. The negative values are interpreted as underestimations of the real-operating conditions, whereas the positive values are interpreted as overestimations of the real-operating conditions.

As shown in Table II, the model with the smallest absolute error provides the unit commitment with the smallest operating costs. For instance, in weeks 2 and 4, the absolute error of the predictions made with the upper boundary model were the lowest among the three compared models, and therefore, the unit commitment had the lowest operating costs, and in weeks 1, 3, and 5, the absolute error of the predictions made with the fuzzy model were the lowest among the three models compared, and therefore, the unit commitment had the lowest operating costs. Thus, despite the adequate performance (in terms of operating costs) of the EMS

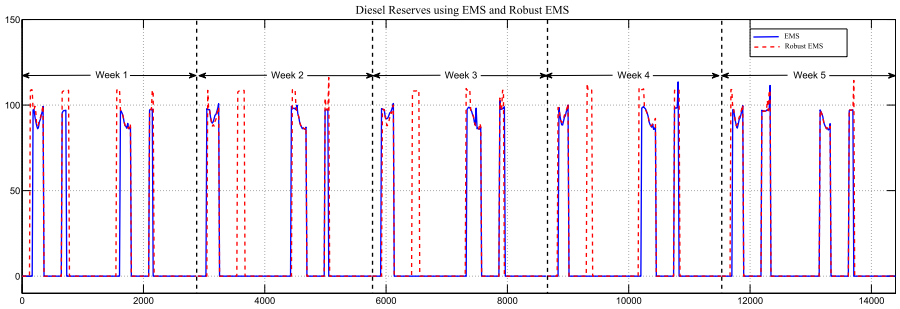


Fig. 3. Comparison between the reserves obtained with the REMS and those with the currently installed EMS in the Huatacondo microgrid.

TABLE II
COMPARISON OF THE OPERATING COSTS USING DIFFERENT MODELS TO PREDICT THE AVAILABLE ENERGY IN THE WIND-BASED ENERGY SOURCES IN THE HUATACONDO MICROGRID

| | Lower | EMS | Upper |
|---|---|---|---|
| Total cost per week | | | |
| 1 | 40739 | 37070 | 37676 |
| 2 | 39898 | 39572 | 37570 |
| 3 | 41577 | 39780 | 42292 |
| 4 | 39414 | 35731 | 34665 |
| 5 | 41756 | 41468 | 42572 |
| Error | | | |
| 1 | −0.612 | −0.035 | 0.283 |
| 2 | −0.670 | −0.211 | 0.054 |
| 3 | −0.572 | 0.457 | 0.842 |
| 4 | −1.280 | −0.612 | 0.288 |
| 5 | −0.440 | 0.175 | 0.964 |

during weeks 1, 3, and 5, in the remaining weeks, the use of the EMS might result in unserved power due to the intermittent behavior of the available energy of the wind-based energy sources. Thus, a significant improvement of the EMS in [3] was achieved using the FPIM as the prediction model. Indeed, as aforementioned, with the use of the FPIM as the prediction model the power balance is satisfied with a confidence level of 95%, despite the variations of the wind power. Note that (in comparison with the EMS) in the Huatacondo microgrid, the increase in the operating costs with the REMS was approximately 4.8% on average. In accordance with the operating costs shown in Table I, the operating costs were lower for the REMS than for the EMS in weeks 2 and 3. The difference between the costs resulted from the number of times the diesel generator was started under each strategy. The lower increase in the operating costs enhanced the cost-effectiveness of the proposed REMS, thus making the proposed EMS suitable for real-microgrid applications.

## V. CONCLUSION

In this paper, an REMS was proposed inside the MPC framework, in which an FPIM was used as the prediction model for the available energy of the NCES in a microgrid. In particular, the wind-based energy sources were modeled using the FPIM, and an adequate representation of the uncertainty in the NCES was achieved. Moreover, the uncertainty of the NCES could eventually be explicitly included in the EMS formulation and thus in the unit dispatch. These accomplishments extend those presented in [3] for the Huatacondo microgrid in the sense that a more reliable operation is possible using the FPIM as the prediction model in the EMS. Furthermore, these accomplishments also extend the applicability of scenario-based formulations to microgrids with a more complex topology and/or with more NCES in the sense that the FPIM can be used to model any NCES and the demand in a microgrid with a reduced number of scenarios. Hence, the resulting REMS is suitable for real-microgrid implementations, particularly in wind-diesel-based microgrids or in microgrids in which the main source of uncertainty (without considering the demand) is wind-based energy sources (as in the case analyzed in this paper). Future work should be directed toward determining how to select the values of the weighting factors and/or toward developing a strategy for their on-line computation based on the available historical data.

## REFERENCES

[1] R. H. Lasseter, "Microgrids," in *Proc. IEEE Power Eng. Soc. Winter Meeting*, vol. 1. New York, NY, USA, Jan. 2002, pp. 305–308.
[2] D. E. Olivares *et al.*, "Trends in microgrid control," *IEEE Trans. Smart Grid*, vol. 5, no. 4, pp. 1905–1919, Jul. 2014.
[3] R. Palma-Behnke *et al.*, "A microgrid energy management system based on the rolling horizon strategy," *IEEE Trans. Smart Grid*, vol. 4, no. 2, pp. 996–1006, Jun. 2013.
[4] J. D. Kueck, R. H. Staunton, S. D. Labinov, and B. J. Kirby, "Microgrid energy management system," Oak Ridge Nat. Lab., Consort. Elect. Rel. Technol. Solut., Berkeley, CA, USA, Tech. Rep. ORNL/TM-2002/242, 2003.
[5] D. E. Olivares, C. A. Canizares, and M. Kazerani, "A centralized optimal energy management system for microgrids," in *Proc. IEEE Power Energy Soc. Gen. Meeting*, San Diego, CA, USA, Jul. 2011, pp. 1–6.
[6] N. Hatziargyriou *et al.*, "Energy management and control of island power systems with increased penetration from renewable sources," in *Proc. IEEE Power Eng. Soc. Winter Meeting*, vol. 1. New York, NY, USA, 2002, pp. 335–339.
[7] Y. Zhang, M. Mao, M. Ding, and L. Chang, "Study of energy management system for distributed generation systems," in *Proc. 3rd Int. Conf. Elect. Util. Deregul. Restruct. Power Technol. (DRPT)*, Nanjing, China, Apr. 2008, pp. 2465–2469.
[8] A. Wieland and C. M. Wallenburg, "Dealing with supply chain risks: Linking risk management practices and strategies to performance," *Int. J. Phys. Distrib. Logist. Manage.*, vol. 42, no. 10, pp. 887–905, Feb. 2012.
[9] L. Zhang and Y. Li, "Optimal energy management of wind-battery hybrid power system with two-scale dynamic programming," *IEEE Trans. Sustain. Energy*, vol. 4, no. 3, pp. 765–773, Jul. 2013.
[10] D. Lu and B. Francois, "Strategic framework of an energy management of a microgrid with a photovoltaic-based active generator," in *Proc. 8th Int. Symp. Adv. Electromech. Motion Syst. Elect. Drives Joint Symp. (ELECTROMOTION)*, Lille, France, Jul. 2009, pp. 1–6.

[11] M. Falahi, S. Lotfifard, M. Ehsani, and K. Butler-Purry, "Dynamic model predictive-based energy management of DG integrated distribution systems," *IEEE Trans. Power Del.*, vol. 28, no. 4, pp. 2217–2227, Oct. 2013.
[12] D. E. Olivares, C. A. Canizares, and M. Kazerani, "A centralized energy management system for isolated microgrids," *IEEE Trans. Smart Grid*, vol. 5, no. 4, pp. 1864–1875, Jul. 2014.
[13] I. Prodan and E. Zio, "An optimization-based control approach for reliable microgrid energy management under uncertainties," in *Proc. IEEE Workshop Integr. Stoch. Energy Power Syst. (ISEPS)*, Bucharest, Romania, Nov. 2013, pp. 4–7.
[14] Y. Zhang, N. Gatsis, and G. B. Giannakis, "Robust energy management for microgrids with high-penetration renewables," *IEEE Trans. Sustain. Energy*, vol. 4, no. 4, pp. 944–953, Oct. 2013.
[15] C. A. Hernandez-Aramburo, T. C. Green, and N. Mugniot, "Fuel consumption minimization of a microgrid," *IEEE Trans. Ind. Appl.*, vol. 41, no. 3, pp. 673–681, May/Jun. 2005.
[16] F. Pilo, G. Pisano, and G. G. Soma, "Neural implementation of microgrid central controllers," in *Proc. 5th IEEE Int. Conf. Ind. Informat.*, vol. 2. Vienna, Austria, Jun. 2007, pp. 1177–1182.
[17] A. Sobu and G. Wu, "Optimal operation planning method for isolated micro grid considering uncertainties of renewable power generations and load demand," in *Proc. IEEE Innov. Smart Grid Technol. Asia (ISGT Asia)*, Tianjin, China, May 2012, pp. 1–6.
[18] B. Zhao, Y. Shi, X. Dong, W. Luan, and J. Bornemann, "Short-term operation scheduling in renewable-powered microgrids: A duality-based approach," *IEEE Trans. Sustain. Energy*, vol. 5, no. 1, pp. 209–217, Jan. 2014.
[19] A. Chaouachi, R. M. Kamel, R. Andoulsi, and K. Nagasaka, "Multiobjective intelligent energy management for a microgrid," *IEEE Trans. Ind. Electron.*, vol. 60, no. 4, pp. 1688–1699, Apr. 2013.
[20] C. Chen, S. Duan, T. Cai, B. Liu, and G. Hu, "Smart energy management system for optimal microgrid economic operation," *IET Renew. Power Gener.*, vol. 5, no. 3, pp. 258–267, May 2011.
[21] I. Škrjanc, S. Blažič, and O. Agamennoni, "Identification of dynamical systems with a robust interval fuzzy model," *Automatica*, vol. 41, no. 2, pp. 327–332, Feb. 2005.
[22] B. Lange, K. Rohrig, F. Schlögl, Ü. Cali, and R. Jursa, "Wind power forecasting," in *Renewable Electricity and the Grid*. London, U.K.: Earthscan, 2007, pp. 95–120.
[23] T. Takagi and M. Sugeno, "Fuzzy identification of systems and its applications to modeling and control," *IEEE Trans. Syst., Man, Cybern., Syst.*, vol. SMC-15, no. 1, pp. 116–132, Jan./Feb. 1985.
[24] A. Cipriano and D. Sáez, "A new method for structure identification of fuzzy models and its application to combined cycle power plant," *Int. J. Eng. Intell. Syst. Elect. Eng. Commun.*, vol. 9, no. 2, pp. 101–108, 2001.
[25] F. Avila, D. Saez, G. Jimenez-Estevez, L. Reyes, and A. Nunez, "Fuzzy demand forecasting in a predictive control strategy for a renewable-energy based microgrid," in *Proc. Eur. Control Conf. (ECC)*, Zurich, Switzerland, Jul. 2013, pp. 2020–2025.

**Felipe Valencia** (M'13) was born in Medellín, Colombia. He received the Master's and Ph.D. (magna cum laude) degrees in control engineering from the Univeridad Nacional de Colombia, Medellín.

He is a Control Engineer with the Universidad Nacional de Colombia. He is currently a Full Time Researcher with the Solar Energy Research Center Solar Energy Research Centre-Chile, Department of Electrical Engineering, University of Chile, Santiago. His current research interests include design of distributed and hierarchical strategies for controlling large-scale systems, researching on different fields such as power energy generation, transmission, and distribution systems, transportation, and smartgrids.

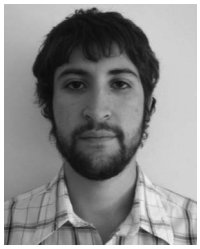

**Jorge Collado** was born in Santiago, Chile. He received the B.Sc. degree in electrical engineering from the University of Chile, Santiago, in 2013.

His current research interests include robust energy management systems and microgrids.

**Doris Sáez** (S'93–M'96–SM'05) was born in Panguipulli, Chile. She received the M.Sc. and Ph.D. degrees in electrical engineering from the Pontificia Universidad Católica de Chile, Santiago, in 1995 and 2000, respectively.

She is currently an Associate Professor with the Department of Electrical Engineering, University of Chile, Santiago. Her current research interests include predictive control, fuzzy control design, fuzzy identification, control of power generation plants, and control of transport systems. She has co-authored the books *Hybrid Predictive Control for Dynamic Transport Problems* (Springer-Verlag, 2013) and *Optimization of Industrial Processes at Supervisory Level: Application to Control of Thermal Power Plants* (Springer-Verlag, 2002).

Dr. Sáez is an Associate Editor of the IEEE TRANSACTIONS ON FUZZY SYSTEMS.

**Luis G. Marín** was born in Florencia-Caquetá, Colombia. He received the Electronic Engineering degree from the Universidad Autónoma de Colombia, Bogotá, Colombia, in 2003, and the M.Sc. degree in information sciences and communications from the Universidad Distrital Francisco José de Caldas, Bogotá, in 2012. He is currently pursuing the Ph.D. degree in electrical engineering with the University of Chile, Santiago, Chile.

His current research interests include predictive control, renewable energy plants, and robust control for microgrids.